

RADAR AND ACOUSTIC OBSERVATIONS DURING VTMX FIELD-CAMPAIGN

Paco Lopez Dekker, Apoorva N. Bajaj and Stephen J. Frasier
 Microwave Remote Sensing Laboratory
 Department of Electrical Engineering
 University of Massachusetts
 Amherst, MA 01003-4410

Abstract—During Oct 2000, the University of Massachusetts participated in the first VTMX field campaign with the deployment of two radars and a sodar. This paper presents an overview of night-time stable boundary layer observations made during this campaign. Radar-detectable activity consists mainly of sporadic brief episodes of turbulence, typically confined to the lowest 200 m of the atmosphere.

I. INTRODUCTION

The first field campaign of the Vertical Transport and Mixing program was held during Oct 2000, in the Salt Lake Valley focusing on processes in the nocturnal boundary layer and during morning and evening transitions. The University of Massachusetts Microwave Remote Sensing Laboratory participated in this campaign with a suite of remote sensing instruments including the Turbulent Eddy Profiler (TEP), which is a 915 MHz volume imaging radar, a high-resolution 2.9 GHz FMCW radar, a Doppler sodar, and sonic anemometers. The stable nocturnal boundary layer is characterized by sporadic, short-lived turbulent events which are believed to be responsible for significant mixing. The degree to which these events can be observed and characterized by high resolution radar instruments is the focus of our participation in the VTMX program.

Our broader objective is to determine the minimum spatial and temporal scales at which useful and reliable remote measurements of turbulence are obtainable with current boundary layer profiler technology. The purpose of the paper is to provide an overview of night-time (stable) boundary layer observations produced by our instruments during this field campaign.

II. INSTRUMENTS DESCRIPTION

TEP (Mead et al., 1998; Pollard et al., 2000) is a 915 MHz volume-imaging Doppler radar designed to image local refractive index fluctuations and their radial velocity structure within a 30 degree cone centered about zenith with an angular resolution of 3.5° and range resolution of 30 m.

Umass' FMCW (Ince et al., 2000) is an S-band radar designed to complement TEP measurements providing 2.5 m

This work was in part supported by the U.S. Department of Energy, under the auspices of the Atmospheric Sciences Program of the Office of Biological and Environmental Research, the U.S. Army Research Office (Environmental Sciences)

height-resolution vertical profiles of the Boundary Layer (BL). Its 3.5° beamwidth approximately matches that of a focused TEP-beam. FMCW reflectivity profiles are produced in real-time which can be used to direct airborne sensors to heights of interest.

The backscattered signal received by both TEP and FMCW is Bragg scattering caused by small fluctuations in the index of refraction of air, and by biological targets such as insects. The former is the one that is mainly of interest for turbulence studies, although insects often act as tracers, helping to identify waves, etc.

For Bragg scattering, the backscattered cross section per unit volume, η , has been found to follow the relationship (Ottersten, 1969)

$$\eta \approx 0.38 C_{n^2} \lambda^{-1/3}, \quad (1)$$

where C_{n^2} is the structure function parameter for the index of refraction of air, and λ , the electromagnetic wavelength. The index of refraction structure function parameter can be expressed in terms of the temperature and water vapor mixing ratio function parameters as (Wyngaard et al., 2001):

$$C_{n^2} = a^2 C_{T^2} + 2ab C_{TQ} + b^2 C_{Q^2}, \quad (2)$$

In practice, with a and b approximately equal to $8.6 \cdot 10^{-7}$ and $-6.7 \cdot 10^{-6}$ respectively, the refractive index is much more sensitive to changes in humidity, and therefore radar reflectivity is mainly a measure of C_{Q^2} . A direct consequence is that, for dry air as typically encountered in the Salt Lake Valley, the signal level received by the radar can be expected to be rather low.

At close range, radar observations range are typically limited by ground-clutter. For the FMCW system, parallax effects and ground-clutter limits observability below 75 m, while for TEP the clutter-dominated region can go as high as 200m.

An Aerovironment 3000 Doppler Sodar system, operating at 2800 Hz, was used to sample atmospheric winds and turbulence, at 10 m intervals, up to 400 m altitude above ground level. Data samples were averaged over 5 minutes to generate wind profiles and acoustic reflectivity images. In contrast to radar reflectivity, acoustic reflectivity is mostly related to C_{T^2} (Neff and Coulter, 1986).



Fig. 1. University of Massachusetts students assembling the TEP receiving array, with the SODAR on the left, the FMCW-antennas on the right and the Wasatch Mountains in the background.

III. EXPERIMENTAL SETUP

These instruments were located at the Salt Lake Visitor Center located along I-80 approximately 5 miles west of the SLC airport in the northwest corner of the valley. The site was far away from some of the more complex terrain features in the valley, avoiding certain local effects such as canyon out-flows, but, due to the proximity to the Salt Lake, more exposed to lake-breezes.

The VTMX campaign covered most of October, but operations were concentrated in 10 Intensive Observation Periods (IOP). FMCW operated from IOP 2 through IOP 10. TEP operated from IOP 2 through IOP 7. The sodar operated on and off during the experiments, as it was also used as an acoustic source for testing TEP in a RASS mode.

IV. OBSERVATIONS

Since FMCW data is processed in real-time, and because it generates a relatively small volume of data, it provides a good tool to preview the collected data. As an example, Figure 2 shows a time-height reflectivity image corresponding to the first four hours of the second IOP, starting at 22:00 UTC on Oct 6 (4 pm local time). This image shows some characteristic features seen throughout the campaign. The period starts with a late afternoon decaying convective boundary layer with a depth of around 400 m. Simultaneously, wave-like structures at a height of about 1200 m AGL can be observed. The last two hours in the period see a large concentration of insects rising at dusk, while little radar-detectable atmospheric activity is present. In the image, a relative reflectivity of 20dB corresponds approximately to an equivalent C_n^2 of 10^{-17} .

We have surveyed hourly FMCW-images to identify active periods. To produce a first, arbitrary classification, we identify hour-periods with radar-detectable activity below

TABLE I
PERCENTAGE OF HOURS WITH FMCW-DETECTABLE ACTIVITY

Height range	Hours with activity (%)
< 200 m	38%
200-500 m	14%
> 500 m	8%
0-2000m	56%

200 m AGL, between 200 and 500 m, and above 500 m. The first group is relevant because TEP cannot see that activity. The second group includes the top of the afternoon CBL. Results of this survey, summarized in Table I, reveal that only 56% of these periods show any atmospheric activity. Most of the activity is concentrated in the lowest 200m. Many hours labeled as *active* actually contain rather brief turbulence episodes, lasting 20-40 minutes.

Most IOPs start with a late afternoon lake breeze, with surface winds around 3 m/s, producing boundary layer depth of around 400 m (as seen by the radar). Wave-like structures about 1200 m AGL are present during several IOPs.

A couple of hours into the IOP, wind direction typically changes, turning into land breeze, with surface winds about 1-2 m/s. During most of the night, only sporadic episodes of activity are observed by the radars, which, as stated, are typically confined to the lowest 200 m of the NBL. About half the activity detected above 200 m corresponds to the evening transition.

During several nights (IOPs 2,4,6,7 and 8), turbulent activity increases in the early morning, several hours before sunrise. The most dramatic example happened on Oct 17 (see Figure 3), when around 12:30 UTC, over an hour before dawn, an intense burst of turbulence near 100 m AGL

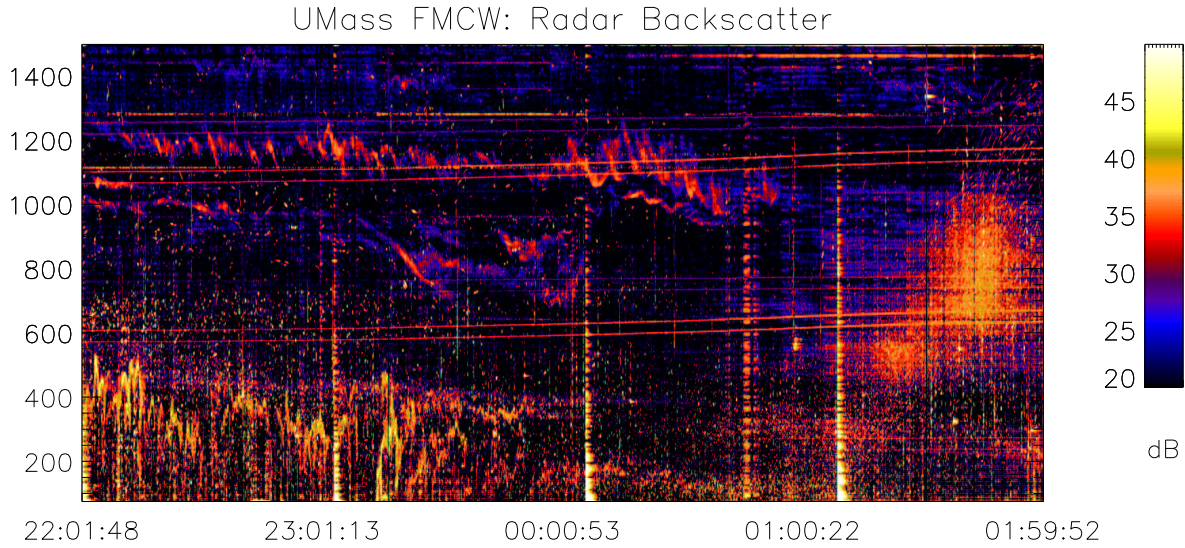


Fig. 2. FMCW time-height reflectivity profile (in relative units). Data corresponds to the first four hours of IOP 2, starting Oct 6 at 22:00 UTC. This image displays several typical features of the VTMX campaign. The first two hours are characterized by the decay of the CBL, with a depth of approximately 400m AGL. Simultaneously, wave-structures can be seen at 1200m. The last two hours in the image show a large concentration of airborne insects (appearing as dots in the image) and very little, if any, detectable atmospheric activity.

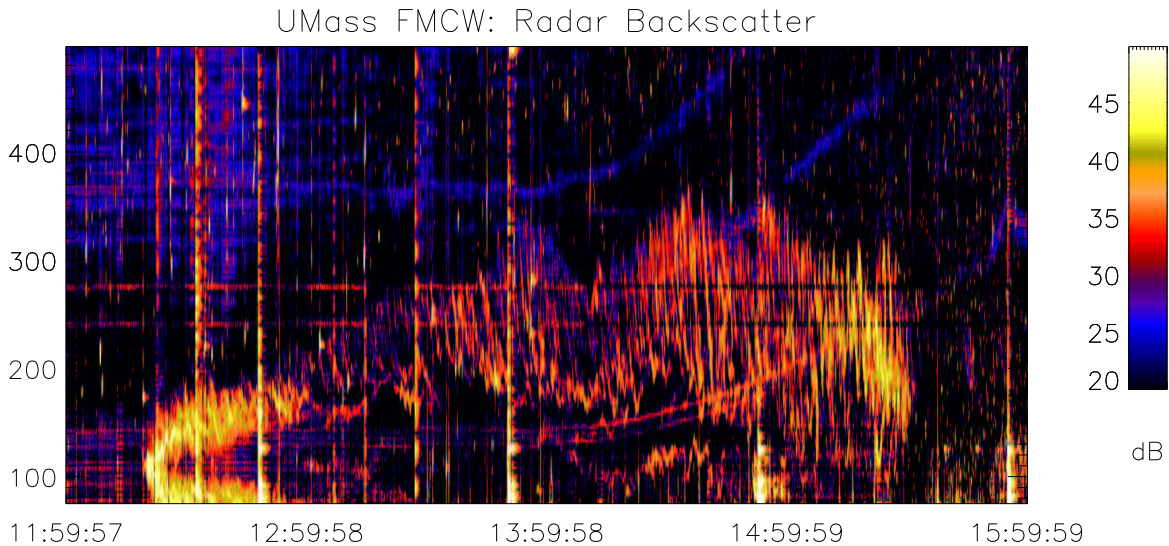


Fig. 3. FMCW time-height reflectivity profile (in relative units). Data corresponds to the first four hours of IOP 6, starting Oct 17 at 12:00 UTC. Around 12:30 UTC, over an hour before sunrise, an intense burst of turbulence appears to split creating a short-lived surface layer and a rising and broadening turbulent layer. Similar events, although weaker and shorter were observed during Oct 9 (IOP 4) and possibly on Oct 18 (IOP 7).

appears to split creating a short-lived surface layer and a rising and deepening turbulent layer. The sonic anemometer also records this event, as can be seen from variances of T and w shown in Figure 5. Events similar to this one, although less intense, are also observed on Oct 9 and Oct 18.

The last two observation periods, a shortened on Oct 21 and a full IOP on the night of Oct 26, stronger winds, around 5 m/s at surface level, resulted in very little radar-

detectable turbulent action.

In addition to radar reflectivity, the sodar produced acoustic reflectivity profiles in the lowest few hundred meters of the BL. As an example, figure 6 shows a time-height acoustic reflectivity image corresponding to IOP 2, showing near-surface activity throughout the night, increasing towards sunrise. Surface winds measured by the sonic anemometer are also shown in the figure. Acoustic reflectivity is strongly related to C_{T^2} , and is therefore at

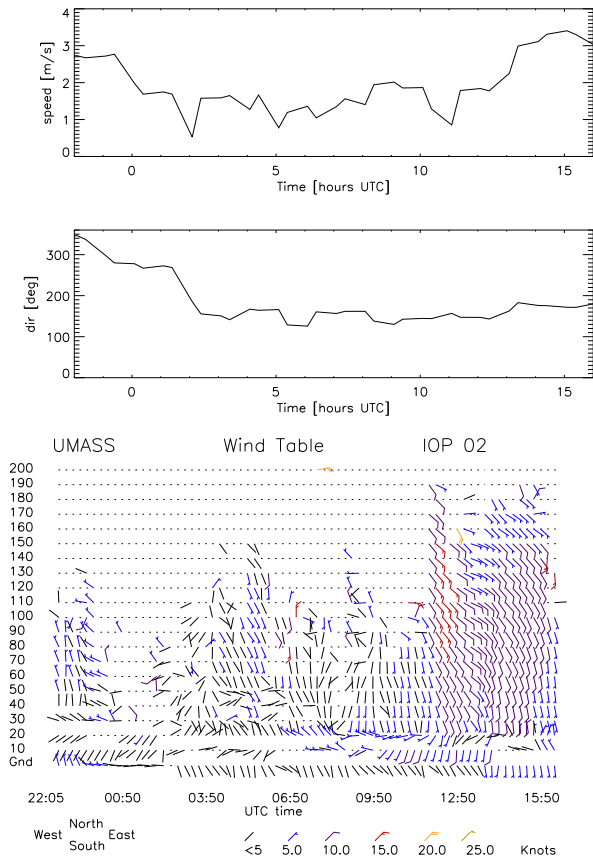


Fig. 4. Wind measurements during IOP 2. The upper two panels show surface wind velocity and direction in degree East of North. Sodar-produced wind-profiles are shown in the lowest panel. The period starts with lake breeze, soon turning into a land breeze, with wind speeds throughout the night of about 1-2 m/s.

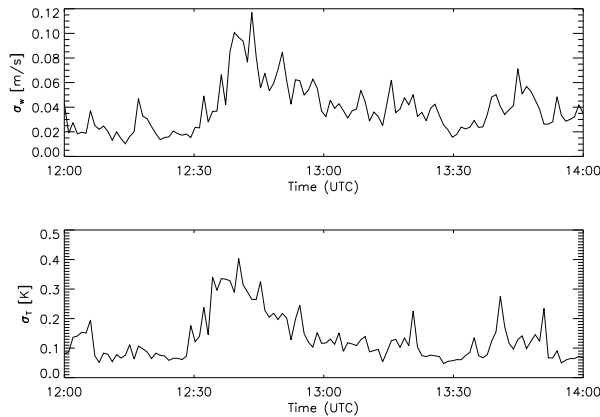


Fig. 5. Surface vertical wind and temperature standard deviations computed over 1-minute periods during IOP 6. At 12:30 UTC the level of measured turbulence suddenly increases, coinciding with the turbulent layer hitting ground, as seen in Figure 3.

least partially independent from radar reflectivity, mostly related to C_{Q^2} . We do in fact see, with a few exceptions, little agreement between the acoustic reflectivity images and radar profiles.

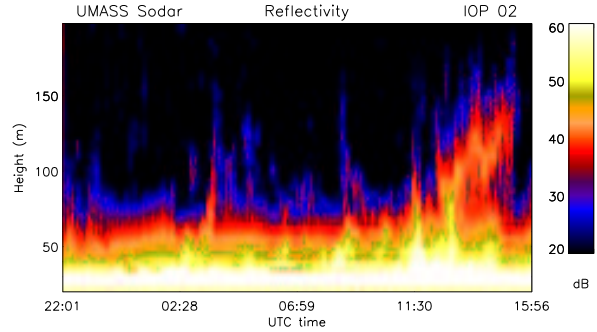


Fig. 6. Time-height image of acoustic reflectivity corresponding to IOP 2, Oct 6-7.

V. CONCLUDING REMARKS

In this paper we have presented a brief overview of the radar and acoustic observations made during the VTMX field campaign. Due to high-altitude cold and dry air encountered during the experiment, radar reflectivity was low, limiting the radar observations. Most night-time turbulent activity is sporadic and confined to the lowest 200 m of the BL.

REFERENCES

Ince, T., Pazmany, A. L., Frasier, S. J., and McIntosh, R. (2000). High resolution profiling of the atmospheric boundary layer. In *Proceedings, 2000 International Geoscience and Remote Sensing Symposium*.

Mead, J., Hopcraft, G., Frasier, S. J., Pollard, B., Cherry, C., Schaubert, D., and McIntosh, R. (1998). A volume-imaging radar wind profiler for atmospheric boundary layer turbulence studies. *J. Atmospheric and Ocean Tech.*, 12:849–859.

Neff, W. and Coulter, R. (1986). *Probing the Atmospheric Boundary Layer*, chapter 13, Acoustic Remote Sensing, pages 201–235. American Meteorological Society.

Ottersten, H. (1969). Atmospheric structure and radar backscattering in clear air. *Radio Science*.

Pollard, B., S.Khanna, S. F., Wyngaard, J., Thomson, D., and McIntosh, R. (2000). Local structure of the convective boundary layer from a volume imaging radar. *J. Atmospheric Sci.*, 57:2281–2296.

Wyngaard, J., Seaman, N., Kimmel, S., and Otte, M. (2001). Concepts, observations, and simulation of refractive index turbulence in the lower atmosphere. *Radio Science*.